Thermo-sensitive P(NIPAm-AA)/nano-SiO2 as Nano Plugging Agent for Shale Gas Drilling Fluids

Weiji Wang [a], Zhengsong Qiu [b], Hanyi Zhong [c], Jianfeng Qu [d], Wenhao Dai [e]

School of Petroleum Engineering, China University of Petroleum, Qingdao 266580, China.

[a]wangweiji2007@126.com, [b]295154512@qq.com, [c]286171554@qq.com, [d]289017063@qq.com, [e]1210838394@qq.com

Abstract

N anotechnology has already contributed significantly to technological advances in energy industry and has the potential to revolutionize the drilling industry. Traditional blocking agents are difficult to form effective mud cake to prevent liquid penetration due to extremely low permeability and tiny pore throat of shales, while nanoscale particles can block shale pore and throat to prevent liquid into formation, thus maintaining wellbore stability and protecting the reservoir. The surface of nano SiO2 particles was modified by silane coupling agent KH570 under ultrasound to introduce vinyl functional group. Through the radical graft copolymerization of thermo-sensitive monomer N-isopropylacrylamide (NIPAm) and hydrophilic monomer acrylic acid (AA) onto the modified surface of KH570- nano -SiO2 nano particles at 80℃, a series of thermo-sensitive poly(NIPAm-AA)/nano-SiO2 composite blocking agents with different lower critical solution temperature (LCST) values were prepared by adjusting the mole ratio between NIPAm and AA and were characterized by FT-IR, TEM and TG. The temperature response behavior was studied by light transmittance test and the sealing performance was studied by the pressure transmission test with Longmaxi formation shale samples. Laboratory investigation showed that the blocking agents with sensitive temperature response behavior had obvious LCST value which arises with the increase of hydrophilic monomer AA. If the temperature was higher than the LCST value of the products the blocking agents played a dual role of physical plugging and chemical inhibition, slowing down pressure transmission remarkably. The surface of shale sealed by the new products presented a hydrophobic property, completely cutting off the water invasion.

Keywords

Nano plugging agent, thermo-sensitive intelligent polymer, wellbore stability, shale gas, drilling fluid.

1. Introduction

At present, shale gas exploration and development has attracted much attention. In view of its accumulation characteristics, extended-reach horizontal well and luster horizontal well were usually adopted to exploit shale gas. Because of the existence of tiny fissures and strong water sensitivity in shale formation, severe wellbore instability is easy to occur in the long horizontal section, which seriously restricts the process of shale gas exploration and development (Wang et al., 2013; Dong et al., 2012; Cui et al., 2011). Shale formation is mainly composed of hard brittle shale, mainly illite and illite smectite mixed layer. For hard brittle shales, pore pressure transmission is the primary cause of wellbore instability. Therefore, the key to maintain wellbore stability is to prevent the transmission of pore pressure. In order to prevent the transmission of pore pressure, an effective sealing of the micropore and microfissure is required. Traditional plugging agents are difficult to form effective mud cake to prevent liquid penetration due to extremely low permeability and tiny pore throat of shales, while nano particles can plug shale pore and throat to prevent liquid into formation, thus improving wellbore stability and protecting the reservoir (Wen et al., 2014; Hamid and Mohammad, 2012; Saeed et al., 2013). In recent 20 years, the research on nano materials has been greatly

developed in many fields. The research of basic theory and application technology of nano optical materials, nano semiconductor, nano biomedical materials, nano enhanced materials, nano modified surface, etc. has made great progress. (Craig and Simon, 2014; Matthew et al., 2014; Lin et al., 2012). The mostly wide research is the combination of smart polymers with environmental response behavior (temperature, pH value, electrolyte concentration, magnetic field strength, electric field strength, etc.) and nanoparticles to realize the intelligence of nanoparticles (Wu et al., 2013; Lian et al., 2015; Muhammad and Bong, 2014). In this study, Nano material technology, intelligent polymer and drilling fluid technology were combined together. The surface of nano SiO_2 particles was modified by silane coupling agent KH570 under ultrasound to introduce vinyl functional group. Then the thermo-sensitive intelligent polymer NIPAm was modified to the surface of SiO_2 nanoparticles, and got thermo-sensitive smart nanoparticles. With the change of temperature, the hydrophilicity and hydrophobicity of nanoparticles surface will change accordingly. Moreover, we can adjust the phase transition temperature of NIPAm by the introduction of hydrophilic monomer and hydrophobic monomer, getting intelligent nanoparticles with different phase transition temperature to adapt to shale formations of different temperature.

2. Experimental

2.1 Materials

SiO_2 nanoparticles (10-20 nm), N-isopropyl acrylamide (NIPAm), were purchased from Aladdin Industrial Corporation and used without further purification. Acroleic acid (AA), Silane coupling agent KH570, Potassium persulfate ($K_2S_2O_8$), Tetrahydrofuran (THF) were purchased from Sinopharm Chemical Reagent Co. Ltd, and used without further purification.

2.2 Synthesis of thermo-sensitive P(NIPAm-AA)/nano-SiO2 nano plugging agent

Surface modification of SiO2 nanoparticles

In brief, 16.23 mmol SiO_2 nanoparticles and 1.02 mmol KH570 were dissolved into 60 mL isopropanol dispersing medium, and adjusted pH value to 7 by adding 1 mol/L NaOH. Then the mixture was ultrasonically dispersed for 30 min. After the above steps, this mixed solution was stirred vigorously and heated up to 85°C, polymerized for 1.5 hours under consecutive ultrasonic shaking. The obtained product was centrifuged at 10000 r/min for 30 min and was washed several times by absolute ethyl alcohol to eliminate the unreacted monomer. After centrifugation, the sedimentation was collected, dried at 60°C, and ground to fine powders. The product was abbreviated as KH570-nano-SiO_2.

Synthesis of thermo-sensitive nano plugging agent

NIPAm and AA in a certain mole ratio (no AA, 90/10, 80/20, 70/30) were dissolved into the mixed solvent of H_2O/THF, with the volume ratio of H_2O/THF to be 2:1, a certain amount of KH570-nano-SiO_2 nanoparticles were also added. Then the mixture was ultrasonically dispersed for 30 min. A certain amount of $K_2S_2O_8$ was added dropwise and heated up to 80°C and deoxygenated with N_2 for 9 hours (shown in Fig. 1). The obtained product was centrifuged at 10000 r/min for 30 min and was washed several times by absolute ethyl alcohol to eliminate the unreacted monomer. After centrifugation, the sedimentation was collected, dried at 90°C, and ground to fine powders for characterization. The product was abbreviated as SD-SEAL.

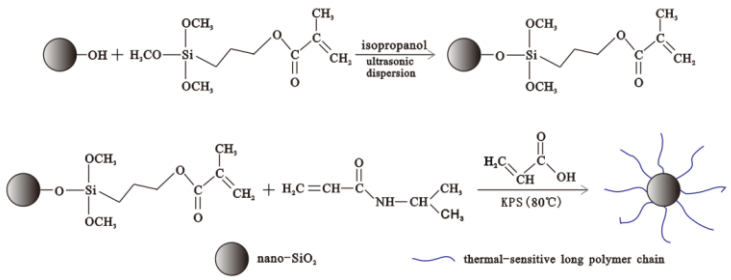

Fig. 1. Synthetic route of nano polymer microspheres intelligent plugging agent

2.3 Characterization

The molecular structure of SD-SEAL was characterized by infrared spectra which were recorded by a Nicolet 6,700 FT-IR spectrometer (NEXUS, USA), scanning from 400 to 4,000 cm^{-1} with a resolution of 4 cm^{-1} in transmission by using KBr pellets. The KBr pellets were prepared by pressing mixtures of 1 mg of powder SD-SEAL and 100 mg of KBr. Transmission electron microscopy (TEM) measurements were acquired with the JEM-2100UHR electron microscope at an accelerating voltage of 200 kV and equipped with a Gatan-832 CCD digital camera. Sample dispersions in water were dropped onto the carbon-coated copper grids and dried in air. Scanning electron microscopy (SEM) measurements were acquired with the Hitachi S-4800 field emission scanning electron microscope (Japan). Thermo gravimetric analysis (TGA) of the SD-SEAL was performed on a SDT Q600 instrument (TA Instrument, USA). The sample was heated at a rate of 20°C/min in nitrogen flow of 50 mL/min.

2.4 Properties test

Temperature responsive behavior

There are a lot of methods to measure the temperature sensitivity of smart polymer. Determining the transmittance of the polymer at different temperatures is the most simple and common method (Feng et al., 2005; Mamoru et al., 2012; Rwei and Nguyen, 2014). When the outside temperature is lower than its LCST value, the smart polymer has a strong hydrophilic property, its water solution is almost transparent, and the transmittance is high. However, when the outside temperature is higher than its LCST value, the hydrophilicity of smart polymer will be changed into hydrophobicity. At this time, micro phase separation will take place, and turbidity will been seen in the mixture, the transmittance is almost zero. Protract the curve of transmittance as a function of temperature, the temperature value corresponding to the inflection point of the curve is the LCST value of the polymer. The temperature responsive behavior of thermo-sensitive nano polymer microspheres intelligent plugging agents with different LCST values were determined by UV VIS spectrophotometer (UV-1,750, SHIMADZU International Trading Co., Ltd.).

Sealing performance evaluation

The pore pressure transmission test was used to measure the physical sealing performance by SD-SEAL nanoparticles on shale permeability using shale hydration measuring (SHM) device shown in Fig. 2 (Xu et al., 2005; Oort, 1994; 1997; Yuan et al., 2012). During pore pressure transmission test, shale cores were subjected to hydraulic gradients when exposing to upstream and downstream fluids. Confining pressure and axial pressure were 5 MPa, upstream pressure was 2.1 MPa and initial downstream pressure was 1.0 MPa. Pore pressure can be tested by testing the variation of downstream pressure. Permeability of shale cores can be calculated using formula (1).

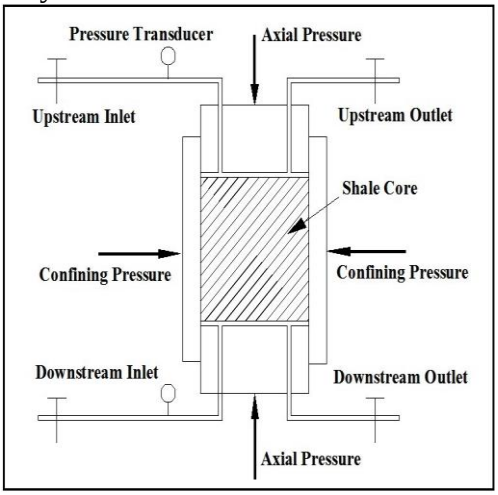

Fig. 2. Shale pressure penetration test apparatus schematic (Xu et al., 2005)

$$K = \frac{\mu\beta VL}{A} \frac{\ln\left(\frac{P_m - P_o}{P_m - P(L,t_2)}\right) - \ln\left(\frac{P_m - P_o}{P_m - P(L,t_1)}\right)}{t_2 - t_1} \quad (1)$$

Where, K is the permeability of shale cores, μm^2; μ is the viscosity of fluids, mPa·s; β is the static compression ratio of fluids, MPa^{-1}; V is the enclosed volume of downstream fluids, cm^3; L is the length of shale cores, cm; A is the cross-sectional area, cm^2; t is total experimental time, s; P_m is the upstream pressure, MPa; P_o is the pore pressure, MPa; P(L, t) is the real-time downstream pressure, MPa.

Shale pore throats deformation characterization

The microscopic morphology of the shale core sealing surface was observed by S-4800 cold-field scanning electron microscope analysis.

3. Results and discussion

3.1 Characterization of SD-SEAL

FT-IR

The FT-IR spectra of SiO_2 nanoparticles and KH570-nano-SiO_2 nanoparticles are shown in Fig. 3(a) and (b). The absorption band at 3,460 cm^{-1} was the associating vibration band of silanol groups and hydrogen bond indicating that there are a lot of OH- on the surface of SiO_2 nanoparticles. The wide absorption band at 3100-3450 cm^{-1} significantly weakened after the surface modification of SiO_2 nanoparticles, The new absorption bands at 2920 and 2851 cm^{-1} are the antisymmetric stretching vibration bands of the methyl and methylene from KH570, 1220 cm^{-1} is the vibration band of ester from KH570. 1108 cm^{-1} and 492 cm^{-1} are the stretching vibration band and bending vibration band of Si-O-Si, indicating that the condensation reaction between SiO_2 nanoparticles and silane coupling agent occurred, silane coupling agent was successfully grafted onto the surface of SiO_2 nanoparticles. The FT-IR spectra of thermo-sensitive P(NIPAm-AA)/nano-SiO_2 is shown in Fig. 3(c). For P(NIPAm-AA)/nano-SiO_2, except for characteristic peaks from KH570-nano-SiO_2, the absorption bands at 3,367 and 3,176 cm^{-1} are N-H bond stretching vibration and absorption peaks. 1,742 cm^{-1} and 1,655cm^{-1} are the characteristic absorption peaks of amide I (C-O bond) and amide Ⅱ (N-H bond). 1,932 cm^{-1} is the association absorption peak of –COOH. Since the product was extracted with acetone, the homopolymers of AA and NIPAm were not included in the product, but the characteristic absorption bands of NIPAm AA and KH570-nano-SiO_2 are obviously observed in the FT-IR spectra. So there are chemical bonds between KH570-nano-SiO_2 and P(NIPAm-AA) polymer chains rather than a simple physical compound. Namely, under the reaction conditions copolymerization reaction took place among KH570-nano-SiO_2 nanoparticles, AA and NIPAm.

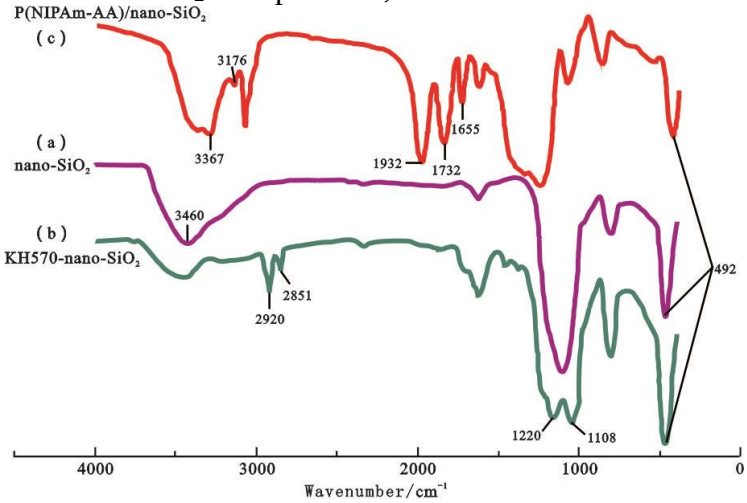

Fig. 3. The IR spectra of different samples

TEM

In order to remove the electrolyte ions of product, we took a small amount of KH570-nano-SiO_2, thermo-sensitive nano plugging agent SD-SEAL in dialysis bag for dialysis. Sample dispersions in water were dropped onto the carbon-coated copper grids and dried in air.

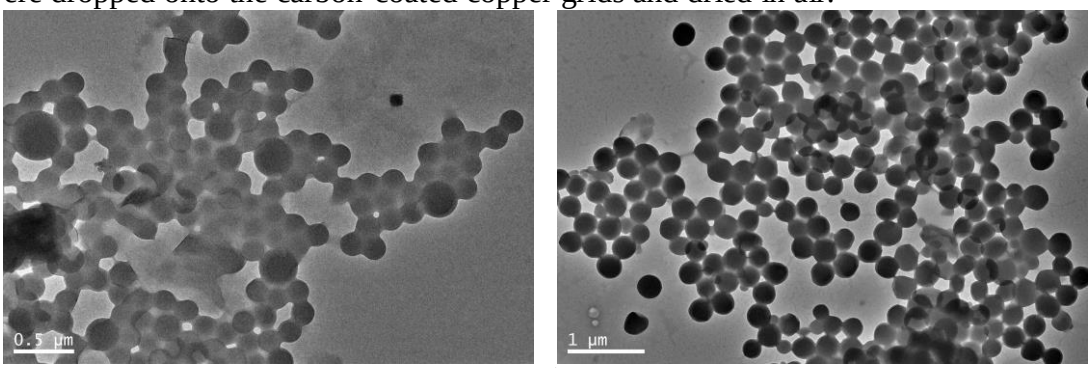

（a）KH570-nano-SiO2 nanoparticles （b）thermo-sensitive P(NIPAm-AA)/nano-SiO2

Fig. 4. The TEM image of different samples

The TEM image of KH570-nano-SiO_2 nanoparticles is presented in Fig. 4(a). KH570-nano-SiO_2 is a hydrophobic nanoparticles, which has poor dispersion in aqueous solution. Irregular shape, uneven particle size, and sticky agglomeration was observed. The TEM image of SD-SEAL is presented in Fig. 4(b). SD-SEAL has good dispersion in aqueous solution with regular shape (mainly spherical) and uniform particle size (about 250 nm). Black spheres are visible in the middle of the SD-DEAL particles, and the surface is covered with a thick gray polymer shell, indicating that thermo-sensitive polymer chain P(NIPAm-AA) had been successfully coated on the surface of KH570-nano-SiO_2 nanoparticles and a product with core-shell structure was obtained.

TGA

The thermal decomposition behaviors of P(NIPAm-AA)/nano-SiO_2 nanoparticles were studied by TGA (Fig. 6). The mass loss curve indicated two major stages. The first stage of mass loss occurs around 200℃ corresponding the evaporation of a small amount of adsorbed water and solvent (Barick, 2010; Mao et al., 2015; Zhong et al., 2015). The second stage is the decomposition of P(NIPAm-AA)/nano-SiO_2 nanoparticles structures around 380℃, indicating that the newly -synthesized thermo-sensitive P(NIPAm-AA)/nano-SiO_2 nanoparticles are high temperature resistant (Bai et al., 2013; Jia et al., 2015; Hugues et al., 2014).

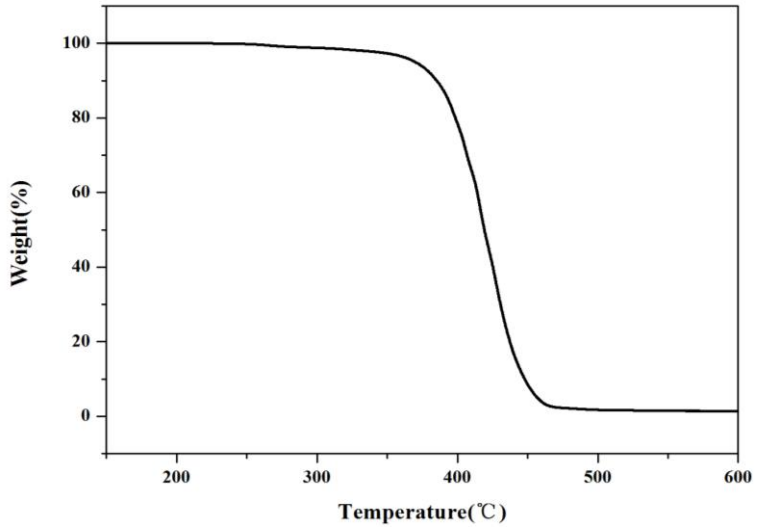

Fig. 6. The TG curves of P(NIPAm-AA)/nano-SiO2 nanoparticles

3.2 Temperature responsive behaviors

The temperature responsive behaviors of thermo-sensitive P(NIPAm-AA)/nano-SiO_2 nanoparticles were studied by transmittance experiment (Fig. 7). Laboratory investigation showed that SD-SEAL

with sensitive temperature response behavior had obvious LCST values, which increase with the increase of hydrophilic monomer AA. Different plugging agents corresponding to NIPAm and AA in a certain mole ratio (no AA, 90/10, 80/20, 70/30) had different LCST values corresponding to 53°C, 63°C, 81°C, 93°C.

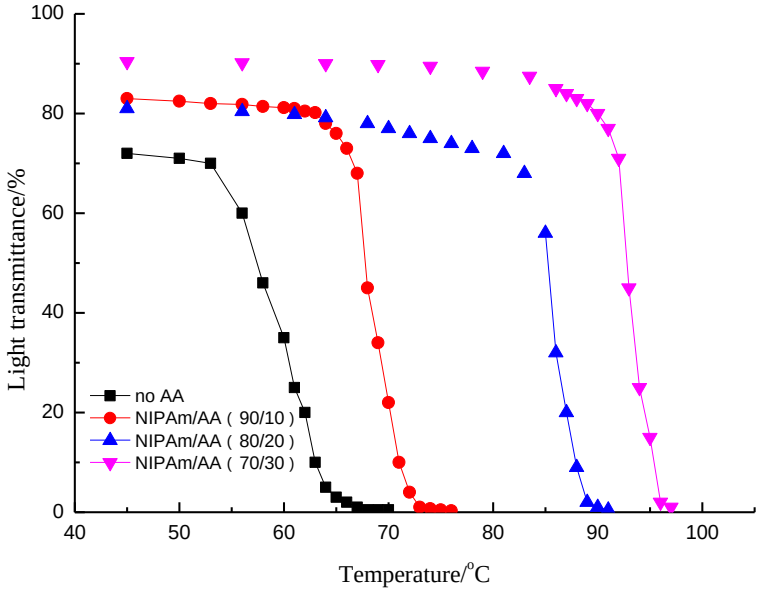

Fig. 7. Transmittance as a function of temperature for nano plugging agent

The main driving force for the phase transition of thermo-sensitive nano sealing agents in aqueous solution is the hydrogen bond effect and hydrophobic effect (Xu et al., 2013; Cong and Doo, 2012; Chen et al., 2013). When temperature was lower than its LCST value, SD-SEAL had a high solubility in water, due to the more polar groups (-CONH- of NIPAm and -COOH of AA) on the molecular chain. These polar groups interact with the surrounding water molecules to form strong hydrogen bonds. Because of the effect of hydrogen bond and Van der Waals' force, the water molecules around the macromolecular chain would form solvation shell which was connected by hydrogen bond and its ordering degree was higher. So that SD-SEAL could be dissolved in water, and the molecular chain could be stretched and linear in water, showing the hydrophilic properties of the whole molecule. But when the solution temperature was above its LCST value, the hydrogen bonds formed between polar groups and water molecules were destroyed, also the solvation layers of the hydrophobic parts of the molecular chain were destroyed, leading an entropy increase of the dispersion system. The hydrophobic association of non-polar group isopropyl was dominant, showing hydrophobic properties of the whole molecule. Water molecules were expelled from the solvation layers causing phase transition. Therefore, with the increase of temperature the regularity of hydrogen bonds was destroyed, the molecules were changed from hydrophilic to hydrophobic.

3.3 Sealing performance evaluation

SEM observation of shale samples

The sealing performance of SD-SEAL was studied by the pressure transmission tests with Longmaxi formation shale samples. The microstructure characteristics of shale samples were observed by scanning electron microscope. As can be seen in Fig. 8, micro-pores were developed in shale matrix, pore size were mainly distributed in 200-800 nm, micro-fractures and bedding were also developed well, the fissure width was 0.5-3 μm.

Pore pressure transmission tests

During the pore pressure transmission tests, the downstream fluid was 4wt% sodium chloride solution, and the upstream fluids were 4wt% sodium chloride solution, or 4wt% sodium chloride solution with 2wt% SD-SEAL. The sealing performance of SD-SEAL was tested at room temperature and temperature above its LCST value (Fig. 9), the microscopic morphology of the core

sealing surface was observed by scanning electron microscope (Fig. 11), also the wettability of the core sealing surface was tested (Fig. 12).

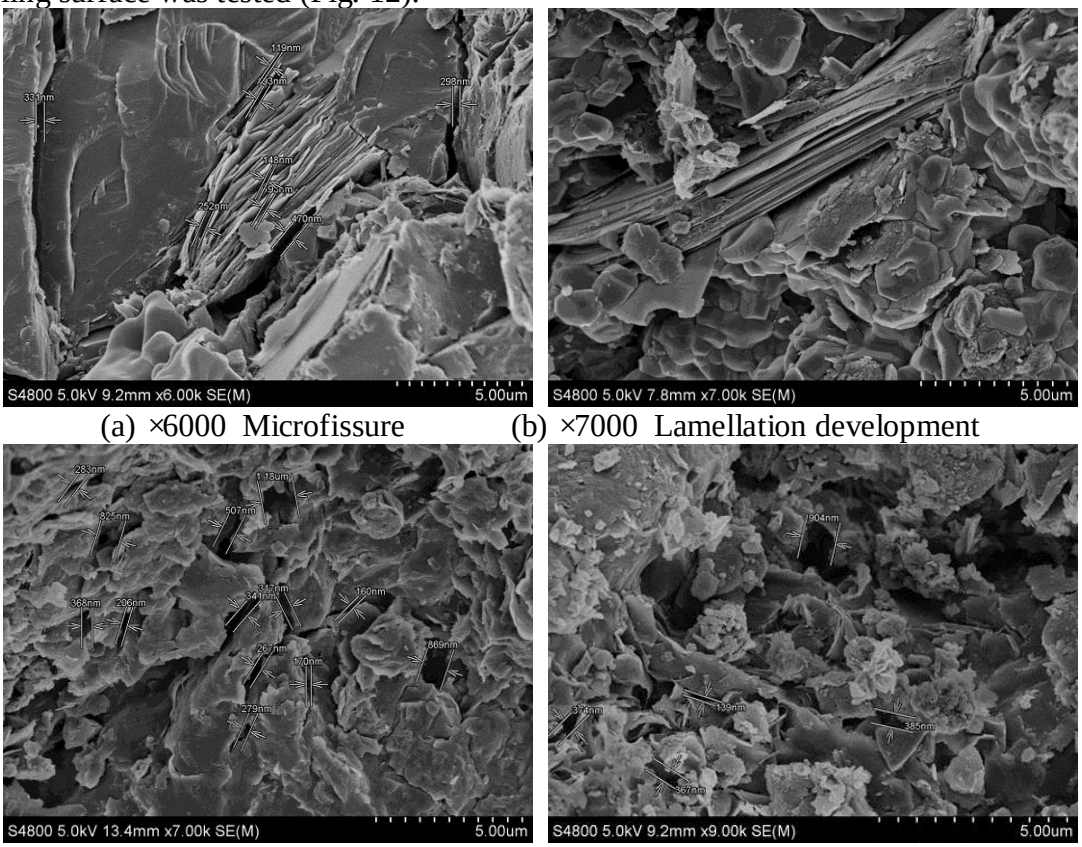

(a) ×6000 Microfissure (b) ×7000 Lamellation development

(c) ×7000 Microfracture and micro pore (d) ×9000 Micro pore

Fig. 8. The SEM images of lungmachi formation shale samples

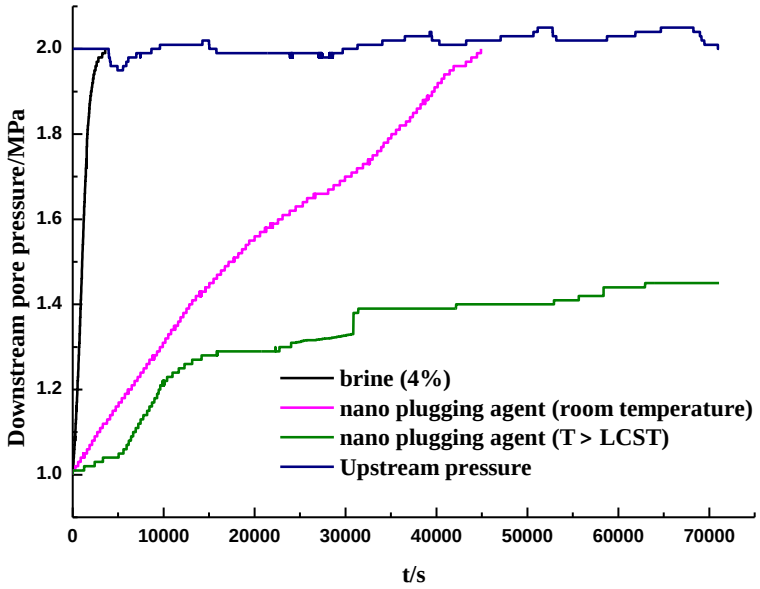

(a) Pore pressure transmission test curves

As can be seen in Fig. 9, the pressure transmission of brine was fast, and 6.5 min later the downstream pressure was almost equivalent to the upstream pressure. At room temperature, the thermo-sensitive nano plugging agent slowed down pressure transmission, reduced shale permeability remarkably. Under the action of pressure, nano particles were pressed into the micro pores and micro fractures of shale surface forming physical sealing layers. The shale permeability was reduced from 3.34×10^{-7} μm^2 to 0.222×10^{-7} μm^2. When the temperature is above its LCST value, the downstream pressure changed less, 4 hours later the pressure transmission curve was close to horizontal line after 4 hours.

The effect of SD-SEAL slowing down pressure transmission and reducing shale permeability was much better. At this moment, the thermo-sensitive polymer of SD-SEAL surface was changed from hydrophilic to hydrophobic. A hydrophobic layer was formed on the shale surface having the effect of chemical inhibition. The shale permeability was reduced from 3.34×10^{-7} μm^2 to 0.081×10^{-7} μm^2. Therefore, when the temperature was higher than its LCST value, SD-SEAL played a dual role of physical plugging and chemical inhibition, which greatly improved the stability of shale (Fig. 10).

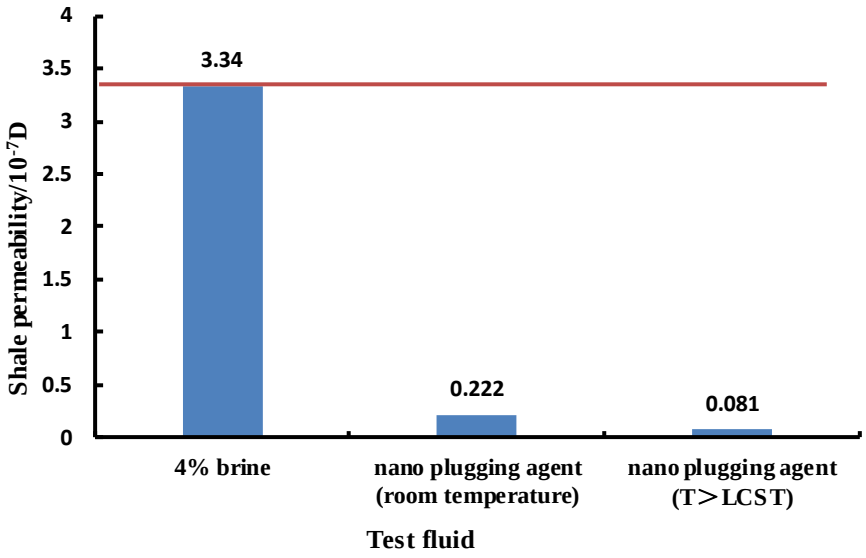

(b) shale permeability

Fig. 9. Pressure transmission test of thermo-sensitive nano plugging agent

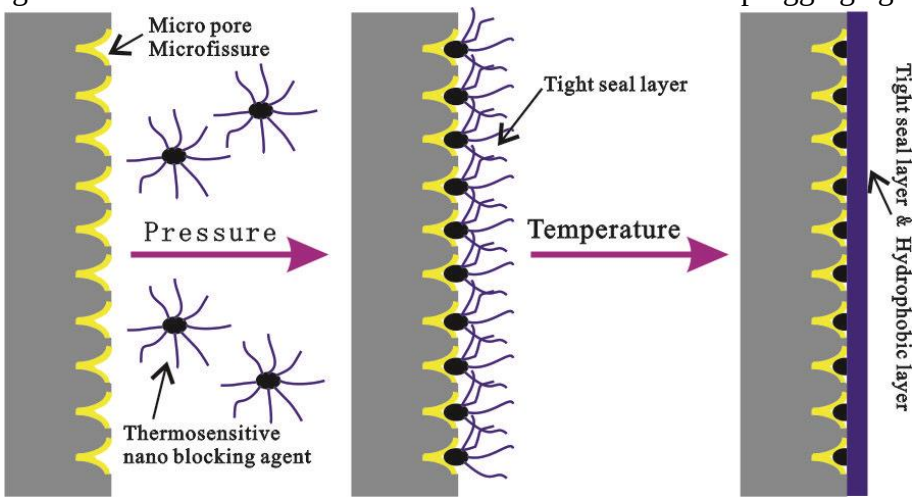

Fig. 10. Schematic diagram of physical plugging and chemical inhibition of SD-SEAL

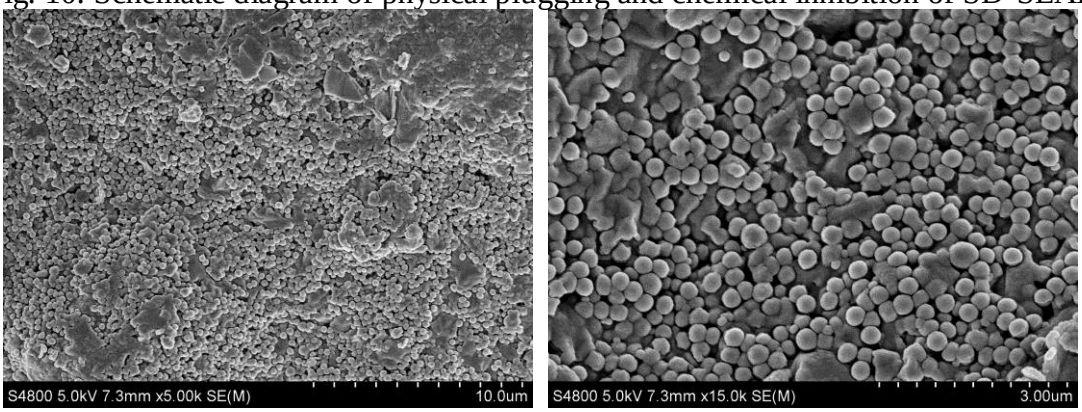

(a) ×5000 (b) ×15000

Fig. 11. The SEM images of sealing surface of shale

The microstructure characteristics of the sealing surface of shale were observed by scanning electron microscope. As can be seen in Fig. 11, after sealed by SD-SEAL the surface of shale was smooth and dense, SD-SEAL tightly packed in the micro pores and micro fractures of shale, spherical particles were clearly visible on the surface of shale. The filling and repairing function of SD-SEAL improved the compaction of core and effectively reduced the permeability.

3.4 Wettability tests

According to the wettability test results (Fig. 12), the surface of shale was complete water wetting before sealing. At room temperature the surface of shale was hydrophilic after sealing, the wetting angle was 40°. When the temperature was higher than its LCST value the surface of shale was hydrophobic, the wetting angle was 125°. Wettability tests further verified the results of pore pressure transmission tests.

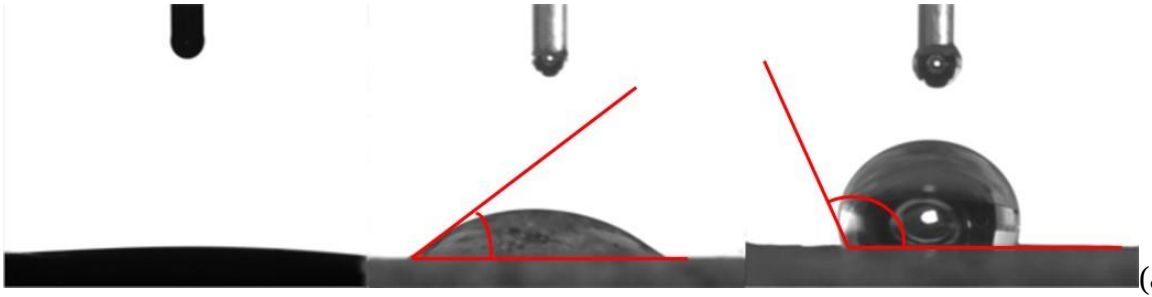

(a) room temperature, before sealing (b) room temperature, after sealing (c) T＞LCST, after sealing

Fig. 12. Wettability test of sealing surface of shale

4. Conclusion

The surface of nano SiO_2 particles was modified by silane coupling agent KH570 under ultrasound to introduce vinyl functional group. Furthermore, through the radical graft copolymerization of thermo-sensitive monomer NIPAm and hydrophilic monomer AA onto the surface of KH570-nano-SiO_2 nanoparticles, a series of thermo-sensitive intelligent plugging agents SD-SEAL with different LCST values were prepared by adjusting the mole ratio between NIPAm and AA. SD-SEAL with sensitive temperature response behavior had obvious LCST value which arises with the increase of hydrophilic monomer AA. Different plugging agents corresponding to NIPAm and AA in a certain mole ratio (no AA, 90/10, 80/20, 70/30) had different LCST values corresponding to 53°C, 63°C, 81°C, 93°C. When the temperature was higher than its LCST value, SD-SEAL played a dual role of physical plugging and chemical inhibition, slowed down pressure transmission and reduced shale permeability remarkably, which greatly improved the stability of shale.

Acknowledgements

We would like to thank the financial support from the National Science Foundation of China (No. 51374233, No. 51474235), the Fundamental Research Funds for the Central Universities (No. 15CX06021A) and the Graduate Student Innovation Project from China University of Petroleum (East China) (No. YCX2015011).

References

[1] Bai X D and Pu X L. The Performance of PMMA Nano-latex in Drilling Fluids [J]. *DRILLING FLUID & COMPLETION FLUID*, 2010, 27(1): 8-10. (in Chinese)

[2] Cui S H, Ban F S and Yuan G J. Status quo and challenges of global shale gas drilling and completion [J]. *NATURAL GAS INDUSTRY*, 2011, 31(04): 72-75. (in Chinese)

[3] Cai J H, Chenevert M E, Sharma M M, et al. Decreasing water invasion into atoka shale using nonmodified silica nanoparticles [C]. 2012, *SPE-146979-PA*.

[4] Craig C and Simon H. Valuing Values: Better Public Engagement on Nanotechnology Demands a Better Understanding of the Diversity of Publics [J]. *NanoEthics*, 2014, 8(1): 55-71.

[5] Chen S L, Liu M Z, Jin S P, et al. pH-/temperature-sensitive carboxymethyl chitosan/poly(N-isopropylacrylamide-co-methacrylic acid) IPN: preparation, characterization and sustained release of riboflavin [J]. *Polymer Bulletin*, 2013, 71(3): 719-734.
[6] Cong T H and Doo S L. Controlling the properties of poly (amino ester urethane)–poly(ethylene glycol)–poly(amino ester urethane) triblock copolymer pH/temperature-sensitive hydrogel [J]. *Colloid and Polymer Science*, 2012, 290(11): 1077-1086.
[7] Dong D Z, Zou C N, Yang H, et al. Progress and prospects of shale gas exploration and development in China [J]. *Acta Petrolei Sinica*, 2012, 33(S1): 107-114. (in Chinese)
[8] Deepti M, Ruma A, Swati L, et al. Synthesis and characterization of iron oxide nanoparticles by solvothermal method [J]. *Protection of Metals and Physical Chemistry of Surfaces*, 2014, 50(5): 628-631.
[9] Farooq M H, Xu X G, Yang H L, et al. Room temperature ferromagnetism of boron-doped ZnO nanoparticles prepared by solvothermal method [J]. *Rare Metals*, 2013, 32(3): 264-268.
[10] Feng X, Chen L, Dong J, et al. Fast responsive temperature-sensitive hydrogel and its application on bioseparation [J]. *Acta Scientiarum Naturalium Universitatis Nankaiensis*, 2005, 38(6): 34-40. (in Chinese)
[11] Hamid R and Mohammad A. Chemo-poroelastic analysis of pore pressure and stress distribution around a wellbore in swelling shale: effect of undrained response and horizontal permeability anisotropy [J]. *Geomechanics and Geoengineering*, 2012, 7(3): 209-218.
[12] Hoelscher K P, Stefano G D, Riley M, et al. Application of nanotechnology in drilling fluids [C]. 2012, *SPE-157031-MS*.
[13] Lin S F, Lin H S and Wu Y Y. Validation and Exploration of Instruments for Assessing Public Knowledge of and Attitudes toward Nanotechnology [J]. *Journal of Science Education and Technology*, 2012, 22(4): 548-559.
[14] Lian Q, Zheng X F and Wang D J. Synthesis of magnetic $Co_{0.5}Zn_{0.5}Fe_2O_4$-chitosan nanoparticles as pH responsive drug delivery system [J]. *Russian Journal of General Chemistry*, 2015, 85(1): 152-154.
[15] Matthew K, Phil M and Sarah R D. Narrative, Nanotechnology and the Accomplishment of Public Responses: a Response to Thorstensen [J]. *NanoEthics*, 2014, 8(3): 241-250.
[16] Muhammad G and Bong G C. Development of pH-responsive chitosan-coated mesoporous silica nanoparticles [J]. *Macromolecular Research*, 2014, 22(4): 412-417.
[17] Mamoru K K, Saigo S and Etsuo K. LCST behavior of copolymers of N-isopropylacrylamide and N-isopropylmethacrylamide in water [J]. *Colloid and Polymer Science*, 2012, 290(16): 1671-1681.
[18] Nguyen T Q and Duong N H. Comparative study of room temperature ferromagnetism in undoped and Ni-doped TiO_2 nanowires synthesized by solvothermal method [J]. *Journal of Materials Science: Materials in Electronics*, 2012, 24(2): 793-798.
[19] Oort E V. A novel technique for the investigation of drilling fluid induced borehole instability in shales [C]. 1994, *SPE-28064*.
[20] Oort E V. Physics-chemical stabilization of shales [C].1997, *SPE-37263*.
[21] Qu Y Z, Sun J S, Su Y N, et al. A Nano Composite Material Poly (styrene -b-acrylamide) /Bentonite: the Laboratory Synthesis and Laboratory Research on the Filtration Control Performance Thereof [J]. *DRILLING FLUID & COMPLETION FLUID*, 2007, 24(4): 15-18. (in Chinese)
[22] Rwei S P and Nguyen T A. Formation of liquid crystals and behavior of LCST upon addition of xanthan gum (XG) to hydroxypropyl cellulose (HPC) solutions [J]. *Cellulose*, 2014, 22(1): 53-61.
[23] Saeed R, Haniyeh J, Cyrus G, et al. Simulation of wellbore stability with thermo- hydro- chemo -mechanical coupling in troublesome formations: an example from Ahwaz oil field, SW Iran [J]. *Arabian Journal of Geosciences*, 2013, 8(1): 379-396.
[24] Wang W F, Liu P, Chen C, et al. The study of shale gas reservoir theory and resources evaluation

[J]. *Natural Gas Geoscience*, 2013, 24(3):429-438. (in Chinese)
[25] Wen H, Chen M, Jin Y, et al. A chemo-mechanical coupling model of deviated borehole stability in hard brittle shale [J]. *PETROLEUM EXPLORATION AND DEVELOPMENT*, 2014, 41(6): 748-754. (in Chinese)
[26] Waleed A B, Muhammed A, Arun R, et al. Nanotechnology Improves Wellbore Strengthening and Minimizes Differential Sticking Problems in Highly Depleted Formation [C]. 2015, *SPE-174859-MS*.
[27] Wu Y P, He S, Guo Z R, et al. Preparation and stabilization of silver nanoparticles by a thermo-responsive pentablock terpolymer [J]. *Polymer Science Series B*, 2013, 55(11): 634-642.
[28] Xu X, Wang k, Gu Y C, et al. Synthesis and characterization of pH and temperature sensitive hydrogel based on poly(N-isopropylacrylamide), poly(ε-caprolactone), methylacrylic acid, and methoxyl poly(ethylene glycol) [J]. *Macromolecular Research*, 2013, 21(8): 870-877.
[29] Xu J F, Qiu Z S and Lv K H. Pressure Transmission Testing Technology and Simulation Equipment for Hydra-Mechanics Coupling of Shale [J]. *ACTA PETRILEI SINICA*, 2005, 26(6), 2115-118. (in Chinese)
[30] Yuan J L, Deng J G, Tan Q, et al. Borehole Stability Analysis of Horizontal Drilling in Shale Gas Reservoirs [J]. *Rock Mechanics and Rock Engineering*, 2012, 46(5): 1157-1164.